Neuropharmacology 89 (2015) 122–135

Contents lists available at ScienceDirect

Neuropharmacology

journal homepage: www.elsevier.com/locate/neuropharm

Eslicarbazepine and the enhancement of slow inactivation of voltage-gated sodium channels: A comparison with carbamazepine, oxcarbazepine and lacosamide

Simon Hebeisen [a], Nuno Pires [b], Ana I. Loureiro [b], Maria João Bonifácio [b], Nuno Palma [b], Andrew Whyment [c], David Spanswick [c, d], Patrício Soares-da-Silva [b, e, f, *]

[a] B'SYS GmbH Analytics, Witterswil, Switzerland
[b] BIAL – Portela & C[a], S.A., S. Mamede do Coronado, Portugal
[c] Neurosolutions Ltd, Coventry CV4 7ZS, UK
[d] Department of Physiology, Monash University, Victoria, Australia
[e] Department of Pharmacology and Therapeutics, Faculty of Medicine, University of Porto, Portugal
[f] MedInUP – Center for Drug Discovery and Innovative Medicines, University of Porto, Porto, Portugal

ARTICLE INFO

Article history:
Received 6 May 2014
Received in revised form
17 August 2014
Accepted 3 September 2014
Available online 19 September 2014

Keywords:
Eslicarbazepine
Carbamazepine
Oxcarbazepine
Lacosamide
Voltage-gated sodium channel
Fast inactivation
Slow inactivation

ABSTRACT

This study aimed at evaluating the effects of eslicarbazepine, carbamazepine (CBZ), oxcarbazepine (OXC) and lacosamide (LCM) on the fast and slow inactivated states of voltage-gated sodium channels (VGSC). The anti-epileptiform activity was evaluated in mouse isolated hippocampal slices. The anticonvulsant effects were evaluated in MES and the 6-Hz psychomotor tests. The whole-cell patch-clamp technique was used to investigate the effects of eslicarbazepine, CBZ, OXC and LCM on sodium channels endogenously expressed in N1E-115 mouse neuroblastoma cells. CBZ and eslicarbazepine exhibit similar concentration dependent suppression of epileptiform activity in hippocampal slices. In N1E-115 mouse neuroblastoma cells, at a concentration of 250 μM, the voltage dependence of the fast inactivation was not influenced by eslicarbazepine, whereas LCM, CBZ and OXC shifted the $V_{0.5}$ value (mV) by −4.8, −12.0 and −16.6, respectively. Eslicarbazepine- and LCM-treated fast-inactivated channels recovered similarly to control conditions, whereas CBZ- and OXC-treated channels required longer pulses to recover. CBZ, eslicarbazepine and LCM shifted the voltage dependence of the slow inactivation ($V_{0.5}$, mV) by −4.6, −31.2 and −53.3, respectively. For eslicarbazepine, LCM, CBZ and OXC, the affinity to the slow inactivated state was 5.9, 10.4, 1.7 and 1.8 times higher than to the channels in the resting state, respectively. In conclusion, eslicarbazepine did not share with CBZ and OXC the ability to alter fast inactivation of VGSC. Both eslicarbazepine and LCM reduce VGSC availability through enhancement of slow inactivation, but LCM demonstrated higher interaction with VGSC in the resting state and with fast inactivation gating.

1. Introduction

Eslicarbazepine acetate (ESL), a once-daily antiepileptic drug (AED) (Almeida and Soares-da-Silva, 2007; Bialer and Soares-da-Silva, 2012), was approved in 2009 by the European Medicines Agency and in 2013 by the Food and Drug Administration as adjunctive therapy in adults with partial-onset seizures (POS). Following oral administration, ESL undergoes extensive first pass hydrolysis to its major active metabolite eslicarbazepine (also known as (S)-licarbazepine) (Elger et al., 2013; Falcao et al., 2007; Perucca et al., 2011), which represents approximately 95% of circulating active moieties. Though ESL, on its own, preferentially

Abbreviations: 4-AP, 4 aminopyridine; AED, antiepileptic drug; CBZ, carbamazepine; Ct, cycle threshold; ΔΔCt, comparative Ct; ECACC, European Collection of Animal Cell Cultures; ESL, eslicarbazepine acetate; LCM, lacosamide; MES, maximal electroshock; OXC, oxcarbazepine; POS, partial-onset seizures; VGSC, voltage-gated sodium channels.

* Corresponding author. Department of Research and Development, BIAL, À Av. da Siderurgia Nacional, 4745-457 S. Mamede do Coronado, Portugal. Tel.: +351 229866100; fax: +351 229866192.
E-mail addresses: pss@med.up.pt, psoares.silva@bial.com (P. Soares-da-Silva).

http://dx.doi.org/10.1016/j.neuropharm.2014.09.008
0028-3908/

blocked voltage-gated sodium channels (VGSC) in rapidly firing neurons (Bonifacio et al., 2001), the *in vivo* effects of ESL may be limited to its extensive conversion to eslicarbazepine. Mechanistically, however, it is important to underline that the affinity of eslicarbazepine for VGSC in the resting state was considerably lower than that of CBZ and oxcarbazepine (OXC), a feature that may translate into an enhanced inhibitory selectivity of eslicarbazepine for rapidly firing "epileptic" neurons over those with normal activity (Hebeisen et al., 2011).

The fundamental properties that enable sodium channels to carry out their physiological roles include rapid, voltage-dependent activation, which often opens the channel, and inactivation (Vilin and Ruben, 2001). Inactivation closes the channel pore and prevents it from reopening until the cell is hyperpolarized. This makes the cell refractory to firing during a long depolarization (Eijkelkamp et al., 2012; Goldin, 2003). There are at least two distinct kinetic classes of inactivation, termed fast and slow. Fast inactivation in VGSC occurs by a "hinged lid" mechanism in which a cytoplasmic region (the inactivating particle) occludes the pore (Goldin, 2003). Slow inactivation is a separate process that does not involve the inactivating particle and may result from a structural rearrangement of the pore (Vilin and Ruben, 2001). Whereas the majority of VGSC blockers used in the treatment of epileptic seizures interfere with the fast inactivation pathway, there is limited information on the pharmacological tools that may influence the slow inactivation of VGSC (Eijkelkamp et al., 2012). Lacosamide (LCM) was shown to act by enhancing slow inactivation of VGSC (Errington et al., 2008), believed to be a new mechanism of action, as other VGSC-blocking AED (CBZ, phenytoin, lamotrigine, OXC) act on fast inactivation (Rogawski and Loscher, 2004).

The present study was aimed to determine the effects of eslicarbazepine, the major active metabolite of ESL, on the fast and slow inactivated states of VGSC endogenously expressed in N1E-115 mouse neuroblastoma cells. To enable the assessment of the antiseizure activity at spanning scales from single cells up to neural circuits, eslicarbazepine was also evaluated in an epileptiform activity model in mouse hippocampal slices where epileptiform electrical activity was induced following exposure to Mg^{2+} free media containing the potassium channel blocker 4 aminopyridine (4-AP) (Lees et al., 2006; Ross et al., 2000). To assess the *in vivo* pharmacodynamics/pharmacokinetic relationship of eslicarbazepine in the context of antiepileptic therapy, the effects of ESL in the mouse maximal electroshock (MES) test, the 6-Hz psychomotor test, and the plasma and brain tissue levels of eslicarbazepine were also evaluated.

2. Materials and methods

2.1. Chemicals and solutions

All reagents were obtained from Sigma unless otherwise indicated. Eslicarbazepine acetate [(−)-(S)-10-acetoxy-10,11-dihydro-5H-dibenzo/b,f/azepine-5-carboxamide], eslicarbazepine [(+)-(S)-10,11-dihydro-10-hydroxy-5H-dibenzo/b,f/azepine-5-carboxamide], (R)-licarbazepine [(−)-(R)-10,11-dihydro-10-hydroxy-5H-dibenzo/b,f/azepine-5-carboxamide], 10,11-dihydrocarbamazepine (used as internal standard), and oxcarbazepine (OXC), were all synthesized in the Laboratory of Chemistry, BIAL − Portela & C[a], S.A., with purities >99.5%. Lacosamide (LCM) was purchased from UCB-Pharma AG as a 200 mg/mL stock solution. Carbamazepine (CBZ) was purchased from Sigma. All drugs, except LCM, were weighted and dissolved using dimethyl sulfoxide to achieve a concentration of 250 mM. The test concentrations were diluted from stock solutions using bath solution shortly prior to the electrophysiological experiments and kept at room temperature when in use. The concentration of solvent was adapted in all test solutions of one set of experiments. The concentration of dimethyl sulfoxide never exceeded 0.4%. For oral administration, ESL was suspended in 0.2% hydroxypropylmethylcellulose (HPMC) in distilled water.

2.2. Animals

Male CD1 (for mouse hippocampal slices) or NMRI (for MES and 6-Hz psychomotor tests and bioanalysis) mice with a body weight range of 25–35 g or 20–29 g, respectively, were stabilized for at least 3 days after delivery in macrolon cages (25 × 19 × 13 cm; 10 animals per cage) on wood litter with free access to food and water. All experiments were performed in laboratories with controlled environmental conditions and at the same time in the morning to avoid circadian variations. All efforts were made to minimize animal suffering, and animal protocols were designed to reduce the number of animals used. Animal care followed United Kingdom, French and Portuguese legislations on the protection of animals used in experimental and other scientific purposes, in accordance with the European Directive 2010/63/EU on the protection of animals used for scientific purposes.

2.3. Cell culture

N1E-115 mouse neuroblastoma cells were obtained from the European Collection of Animal Cell Cultures (ECACC). The cells were continuously grown in a 1:1 mixture of Dulbecco's modified eagle medium and nutrient mixture F-12 with L-glutamate supplemented with 9% foetal bovine serum and 0.9% Penicillin/Streptomycin solution. Cells were maintained at 37 °C in a humidified atmosphere with 5% CO_2 (rel. humidity about 95%) and passaged at a confluence of about 70–80%. For electrophysiological experiments N1E-115 cells were cultivated on 35 mm culture dishes at a confluence that enabled recording from single cells. Cells were used for patch-clamp experiments 24–72 h after passaging.

2.4. Molecular biology

The identification and quantification of the VGSC expressed in N1E-115 cells (at passage 31), was carried out by real-time PCR using specific TaqMan® Assays (Applied Biosystems). Reverse transcription of total RNA into cDNA was performed using the High Capacity cDNA Archive Kit. For testing the specificity of the assays specific sodium channel cDNA was purchased from Origene. The RNA extraction of cultured N1E-115 cell pellet was performed with the MagNa Pure Compact RNA Isolation Kit (Roche). 500 ng of total RNA was reverse-transcribed in a reaction volume of 100 µl. The incubation protocol was 10 min at 25 °C, then 120 min at 37 °C using a PCR thermocycler for accurate temperature control (GeneAmp PCR System 2700, Applied Biosystems). Quantitation of the target and reference gene expression levels was done using the TaqMan® real-time PCR technology. The real-time PCR mastermix was composed of 2× "qPCRMasterMix" (Eurogentec), ultrapure water, cDNA and the specific assay components. The measurement of the DNA samples was carried out in duplicates, in a 96-well plate format on the ABI PRISM 7700 real-time PCR instrument (Applied Biosystems), with the standard thermal cycling program for TaqMan® Assays. Prior amplification the sample cDNA was diluted 1:10 in H_2O ultrapure. Data analysis was done using the SDS 2.2.2 software (Applied Biosystems) by applying the "automatic baseline" mode. The threshold value was set manually at 0.1. The calculation of the obtained cycle threshold (Ct) values into relation gene expression was performed using the comparative Ct (ΔΔCt) method (ΔΔCt = ΔCt sample − ΔCt calibrator). DNase I was used as housekeeping gene. The resulting relative gene expressions were compared to NaV1.1.

2.5. Electrophysiology

For the experiments in mouse hippocampal slices, mice were cervically dislocated and decapitated; the brain was removed and sectioned into 300 µm thick slices using a Leica VT1000 S (Leica Microsystems UK). Slices were maintained in aCSF equilibrated with 95% O_2–5% CO_2 at room temperature for at least 1 h post-slicing before recording. Individual slices were transferred to a custom-built chamber continuously perfused with equilibrated artificial cerebrospinal fluid (aCSF) at a rate of 4–10 ml/min. This aCSF was of the following composition (mM): NaCl, 127; KCl, 1.9; KH_2PO_4, 1.2; $CaCl_2$, 2.4; $MgCl_2$, 1.3; $NaHCO_3$, 26; D-glucose, 10. Whole-cell recordings were performed at room temperature (17–21 °C) using the 'blind' version of the patch-clamp technique from neurons located in the CA1/CA2 region of the hippocampus with patch pipettes of resistances 4–10 MΩ filled with the following solution (mM); potassium gluconate, 140; KCl, 10; EGTA-Na, 1; HEPES, 10; Na_2ATP, 2; pH 7.4. The non-cytotoxic dye Lucifer yellow (dipotassium salt; 1 mg/ml) was routinely included in the pipette solution to enable retrospective confirmation of recording sites and morphological examination of neurons. Neuronal input resistances were measured by injecting a series of rectangular-wave current pulses of variable amplitude in control conditions and, subsequently, in the presence of test compounds. Recordings were monitored on an oscilloscope and stored on digital audio tapes for later off-line analysis. In addition, data was filtered at 2–5 kHz, digitized at 2–10 kHz (Digidata 1322, Axon Instruments) and stored on a PC running pCLAMP 8.2 data acquisition software. Epileptiform activity in isolated hippocampal slices was induced by exposure of the tissue slice to a bathing medium in which magnesium was omitted and 4-AP (100 µM) included. Quantification was made on the basis of changes in the frequency of action potential firing and, where appropriate, the frequency of bursts compared with baseline values. Analysis of vehicle control slices was also performed.

Culture dishes with N1E-115 cells (between passages 32 and 46) were placed on an inverted microscope and analysed using the patch-clamp technique in the whole-cell configuration. For recording an EPC-9 or EPC-10 patch-clamp amplifier (HEKA) in combination with PatchMaster software (HEKA) was used. During the entire experiments cells were continuously superfused with extracellular solution (137 mM NaCl, 4 mM KCl, 1.8 mM $CaCl_2$, 1 mM $MgCl_2$, 10 mM HEPES, 10 mM Glucose,

pH (NaOH) 7.4). Micropipettes were fabricated on a Narishige P-10 Micropipette puller from Borosilicate glass tubing (Warner Instruments). Pipettes had a tip resistance of typically 4–6 MΩ when filled with an intracellular solution containing 120 mM CsF, 10 mM TEA Chloride, 10 mM NaCl, 1 mM $CaCl_2$, 1 mM $MgCl_2$, 11 mM EGTA, 10 mM HEPES, pH (CsOH) 7.3. The Whole-Cell capacitance was compensated and serial resistance compensation (>70%) was applied. Before each experiment, culture medium was removed from the culture dish containing N1E-115 cells and was replaced by extracellular solution. Only single cells were used for patch-clamp experiments. After forming a Gigaseal between the patch pipette and the cell membrane, the cell membrane across the pipette tip was ruptured to assure electrical access to the cell interior (whole-cell patch-configuration). Cells were held at −80 mV for at least 2 min before voltage protocols were recorded. For analysis only cells exhibiting peak current amplitudes of more than 500 pA when depolarized to −10 mV under control conditions were used. All experiments were performed at room temperature.

2.6. Maximal electroshock test

Male NMRI mice ($n = 12$ per group) were administered MES (50 mA, rectangular current: 0.6 ms pulse width, 0.4 s duration, 50 Hz) via corneal electrodes connected to a constant current shock generator (Ugo Basile 7801) and the number of tonic convulsions recorded. Vehicle (0.2% HPMC in distilled water) and ESL or CBZ were administered orally, at a volume of 10 ml/kg body weight, 60 min before the test.

2.7. 6-Hz psychomotor test

In the 6-Hz psychomotor seizure test, animals ($n = 15$ per group) were administered a rectangular current (pulse: 0.2 ms, 6 Hz, 44 mA for 3 s) via corneal electrodes connected to a constant current shock generator. The resulting seizures were scored 0 (absence of clonus), 1 (forelimb clonus moderate) or 2 (bilateral forelimb clonus with rearings high) during the first minute following current administration. Vehicle (0.2% HPMC in distilled water) and ESL or CBZ were administered orally, at a volume of 10 ml/kg body weight, 60 min before the test. Tests were performed blind.

2.8. Rotarod test

The rotarod test was conducted in mice ($n = 10$ per group) trained to hold onto the rotarod apparatus (Ugo Basile 7650) until they maintain equilibrium for 3 min while rotating at 15 rpm. The number of animals which drop off the rod was counted. Vehicle (0.2% hydroxypropylmethylcellulose in distilled water) and ESL or CBZ were administered orally, at a volume of 10 ml/kg body weight, 60 min before the test.

2.9. Blood sampling and brain collection

In satellite experiments, naive NMRI mice were used for blood sampling and brain collection. For each dose of ESL, 5 mice were orally dosed and sacrificed 60 min post-dosing by decapitation. The blood was collected into heparinised plastic vials and well shaken before being placed in ice. Samples were then centrifuged at 1500 rpm for 5 min, with 200 μl plasma collected from each sample. The plasma and brain samples were placed into plastic vials stored in a freezer (−80 °C) until analysis.

2.10. Analysis of ESL and metabolites

Brain and plasma concentrations of ESL, eslicarbazepine (R)-licarbazepine and OXC were determined using a validated enantioselective LC–MS/MS assay, as previously described (Loureiro et al., 2011). Plasma samples (100 μl) were added with 400 μl of internal standard (ISTD) working solution (2000 ng/ml of 10,11-dihydrocarbamazepine in phosphate buffer pH 5.6) and then processed by solid phase extraction. After thawing and weighing, 0.1 M sodium phosphate buffer (pH 5.6) was added to the brain samples to give a tissue concentration of 0.1 g/ml. The samples were then homogenized using a Heidolph DIAX 900 mixer and transferred to 10 ml plastic centrifugation tubes. After centrifugation at 10,000 *g* for 30 min at 4 °C, 0.5 ml of supernatants were added to 0.5 ml ISTD working solution and then processed by solid phase extraction. The samples were placed on an automatic liquid handler (ASPEC-XL4, Gilson) for solid phase extraction using Oasis, HLB (30 mg, Waters), pre-conditioned with 1 ml of acetonitrile and washed twice with 1 ml of water. Specimens (400 μl) were loaded onto the cartridges and washed twice with 1 ml of water. After the second wash the cartridges were flushed with an air push and then eluted twice with 200 μl of methanol The eluted sample was evaporated until dryness and resuspended into 200 μl of hexane:2-propanol (90:10, v:v). The samples were injected (20 μl) into a LC–MS/MS (Quattro Ultima, Waters) with positive ion detection mode. Separation was performed on a ChiralCel 0.46 cm × 15 cm OD-H column (Chiral technologies, Europe). The mobile phase consisted of an isocratic mixture of hexano:ethanol (80:20, v:v; flow rate of 1 ml/min), and ethanol with 5 mM ammonium acetate (added post-column using a flow rate of 0.15 ml/min). A volume of 20 μl was injected and the column temperature kept at 50 °C for the run time of 7 min. Electrospray ionization was used for all mass spectrometer methods with a cone voltage of 40 V and capillary current of 3.8 kV. The multiple reaction monitoring pair was m/z 239.1 → 194, collision 40 eV for ISTD; 253.1 → 208, collision 25 eV for oxcarbazepine; 255.1 → 194, 237, collision 30 eV for eslicarbazepine and (R)-licarbazepine; 297.1 → 194, 237, collision 30 eV for eslicarbazepine acetate. The autosampler cooler was maintained at 10 °C. The samples were quantified with accuracy and precision over the analytical range of 0.2–8.0 nmol/ml for plasma and 2.0 nmol/g–80 nmol/g for brain. The limit of quantification was 0.2 nmol/ml and 2.0 nmol/g, for plasma and brain respectively.

2.11. Data analysis

Data were analysed using FitMaster software (HEKA), Clampfit (Axon Instruments), SigmaPlot (Systat Software) and Prism (GraphPad Software). Error bars in figures represent standard error mean (SEM). Concentration response curves were fit with a sigmoidal two-parameter equation: current $_{\text{relative peak}} = 100/(1 + (X/IC_{50})^H)$ where X is the drug concentration, IC_{50} is the concentration of drug at half maximal inhibition and H is the Hill coefficient. For the generation of activation curves the conductance (g) was calculated by $g = I/V - E_R$, where I is the peak current amplitude, V the applied voltage and E_R the observed reversal potential. Activation as well as inactivation curves were fit with a Boltzmann function. $I/I_{max} = 1/(1 + \exp((V_{0.5} - V)/k))$, where I_{max} is the maximal conductance or current amplitude, $V_{0.5}$ is the voltage at which the half maximal current or conductance occurs, k is the slope factor and V the test potential. To fit the slow inactivation curves a modified Boltzmann function was used, respecting a constant residual current amplitude. The time courses entering the slow inactivated state and the recovery from the slow inactivated state were fit with a monoexponential function: $I(t) = A_1(1 - \exp(-\tau^* t)) + A_2$, where t is time, A_1 the amplitude of the time depended component and A_2 the time independent amplitude. The time course of the recovery from the fast-inactivated state was fit with a biexponential function without a time independent component. For the analysis of use dependence of anticonvulsant drugs on VGSCs, the time course of peak current amplitudes was fit with a biexponential function with a time independent fraction. Data were statistically analysed with a non-parametric multisample analysis (ANOVA followed by Dunnett's test). Data from the MES test were analysed using Fisher's Exact probability test. ED_{50} values, from corresponding dose–response curves, are presented as mean with 95% confidence intervals (95% CI). Statistical comparisons concerning experiments in mouse hippocampal slices were made between treatment groups where possible using paired or unpaired Student's t-test. P-values less than 0.05 were regarded as statistically significant.

3. Results

3.1. Mouse hippocampal slices

The induction and development of epileptifom activity in mouse hippocampal slices following exposure to Mg^{2+}-free/4-AP bathing medium was characterized by an initial membrane hyperpolarization and large amplitude spontaneous inhibitory postsynaptic potentials (IPSPs) (Fig. 1A and B). This phase progressively diminished over a period of several minutes. A subsequent increase in spontaneous excitatory postsynaptic potentials (EPSPs) which ultimately gave rise to spontaneous action potential firing and/or bursts of action potentials superimposed on depolarizing shifts in membrane potential (Fig. 1C and D). Establishing a baseline level of spontaneous epileptiform activity took between 10 and 30 min (Fig. 1E). Simultaneous paired recordings from two neurones in close proximity revealed synchronized spontaneous bursts of activity characteristic of epileptiform activity (Fig. 1F). Following establishment of a baseline level of epileptiform activity, bath application of increasing concentrations of CBZ induced a suppression of epileptiform activity (Fig. 1G). The mean spontaneous firing frequency in Mg^{2+}-free/4-AP bathing medium was reduced from a baseline value of 0.50 ± 0.36 Hz ($n = 4$) to 0.17 ± 0.07 Hz ($n = 4$, not significant), 0.09 ± 0.09 Hz ($n = 3$, not significant) and completely blocked ($n = 4$, $P < 0.05$) in the presence of 30, 100 and 300 μM CBZ, respectively. Under Mg^{2+}-free/4-AP conditions, mean input resistance was 270 ± 27 MΩ, which was reduced to 261 ± 42 MΩ in the presence of 300 μM CBZ ($n = 3$, not significant). Testing the same concentrations of eslicarbazepine induced similar effects (Fig. 1H). The mean spontaneous firing frequency in Mg^{2+}-free/4-AP bathing medium without eslicarbazepine was 0.39 ± 0.07 Hz ($n = 6$) and this was reduced to 0.31 ± 0.06 Hz ($n = 5$, $P = 0.07$), 0.21 ± 0.04 Hz ($n = 5$, $P = 0.05$) and 0.22 ± 0.14 Hz ($n = 3$,

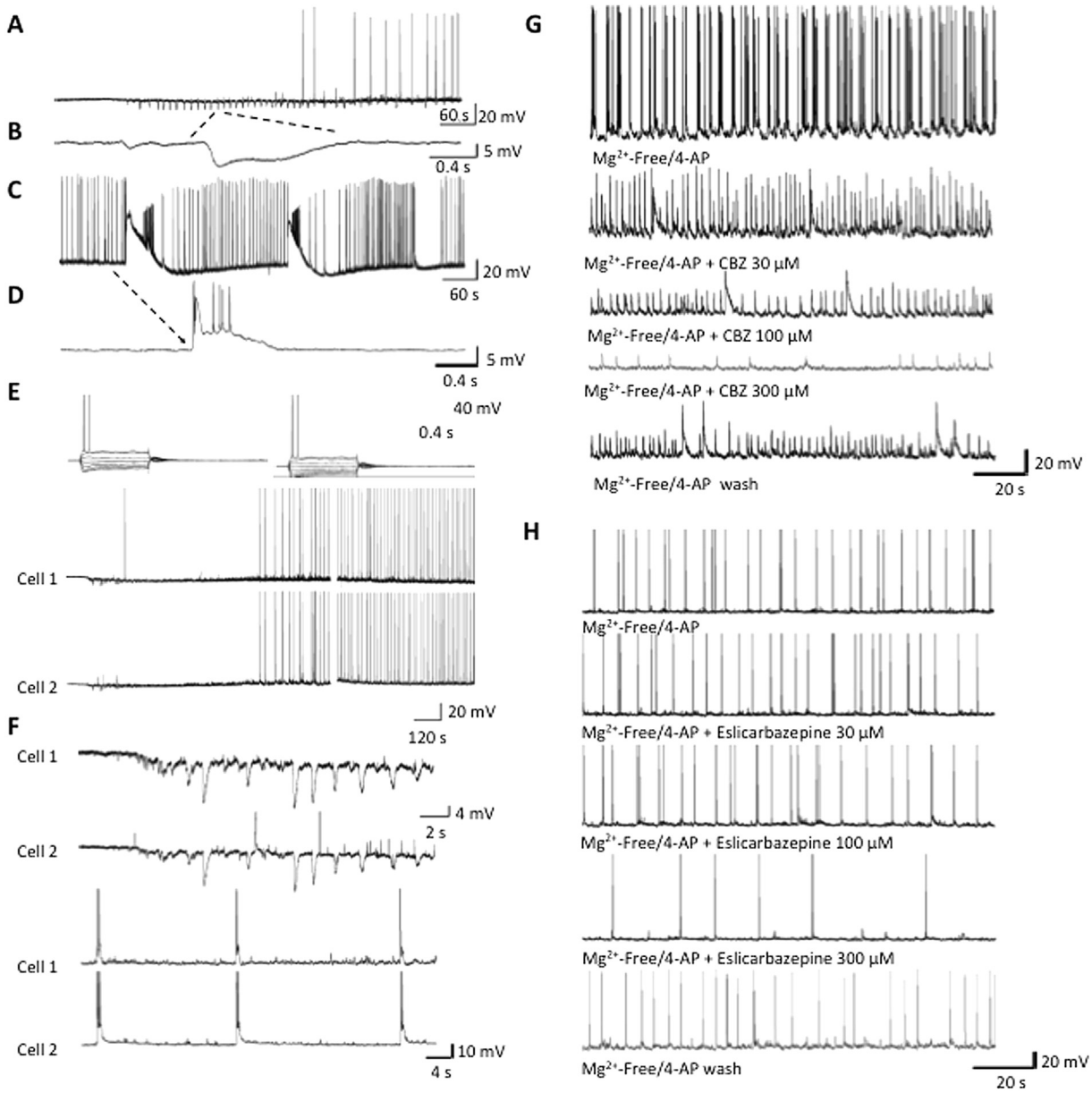

Fig. 1. Samples of a continuous whole-cell current clamp recording showing induction of spontaneous activity following exposure to Mg^{2+}-free/4-AP bathing medium. Note the initial induction of IPSPs (A) (downward deflections, shown on a faster time-base below (B)) followed by an increase in spontaneous firing and bursts of action potentials superimposed on depolarizing shifts (C) shown a faster time-base below (D). Panel E shows samples of a continuous simultaneous paired recording (voltage–current relations shown above) illustrating exposure to Mg^{2+}-free/4-AP-induced synchronous membrane hyperpolarization and IPSP induction in the first instance followed subsequently by membrane depolarization and the induction of synchronous bursts of action potentials. Panel F shows samples of a continuous simultaneous paired recording (same cells as shown in E) showing synchronous IPSPs (above) and subsequently synchronous bursts of firing (below) on a faster time-base. Panels G and H show samples of a continuous whole-cell recording suppression of epileptiform activity, evoked following exposure to Mg^{2+}-free/4-AP bathing medium (control), by increasing concentrations of CBZ (G) and eslicarbazepine (H).

ns) in the presence of 30, 100 and 300 µM eslicarbazepine, respectively. Voltage-current relations were investigated to identify conductance changes associated with eslicarbazepine-induced responses. Eslicarbazepine had no significant effect on neuronal input resistance. Pooled data showed eslicarbazepine induced a change from 197 ± 51 MΩ ($n = 4$) in the Mg^{2+}-free/4-AP bathing medium to 258 ± 83 MΩ ($n = 4$) in the presence of eslicarbazepine.

3.2. Maximal electroshock test

Male NMRI mice were administered MES (50 mA, rectangular current: 0.6 ms pulse width, 0.4 s duration, 50 Hz) via corneal electrodes connected to a constant current shock generator (Ugo Basile 7801) and the number of tonic convulsions recorded. ESL and CBZ demonstrated a similar dose-dependent decrease in MES-induced seizures (with ED_{50} values of 23.0 ± 1.9 and 13.5 ± 2.1 mg/kg, respectively) (Fig. 2A).

3.3. 6-Hz psychomotor test

In the 6-Hz psychomotor seizure test animals were administered a rectangular current (pulse: 0.2 ms, 6 Hz, 44 mA for 3 s) via corneal electrodes connected to a constant current shock generator. The resulting seizures were scored 0 (absence of clonus), 1

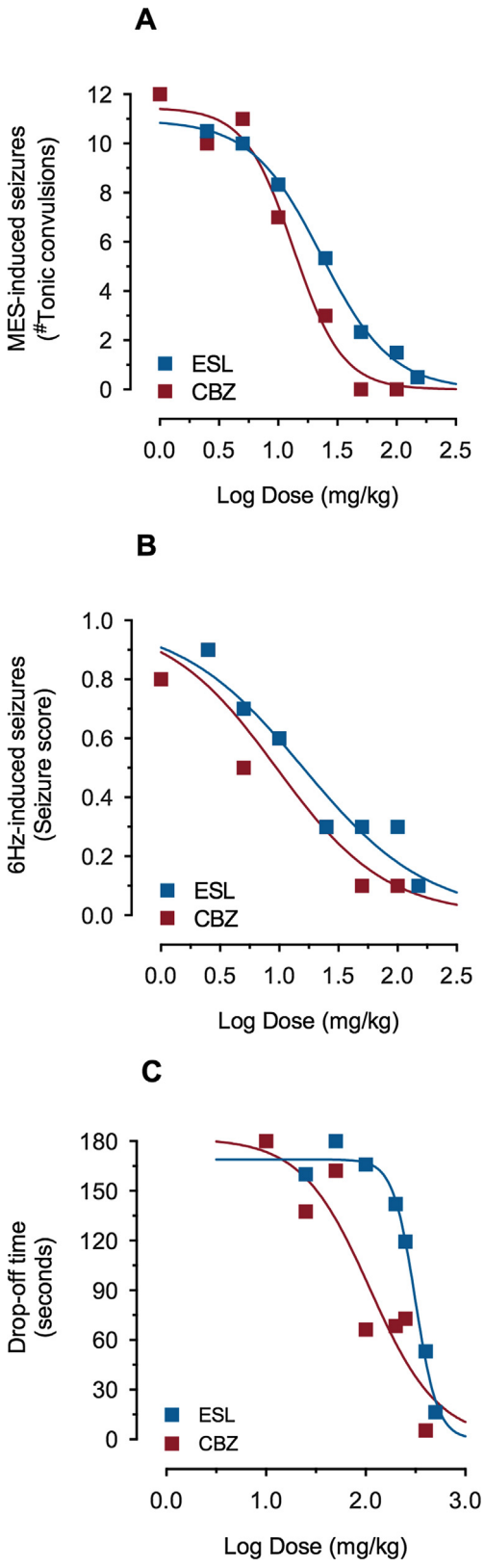

Fig. 2. Anticonvulsant dose–response curves for ESL and CBZ expressed as number of tonic convulsions in the (A) mouse MES test and (B) the mouse 6-Hz psychomotor seizure model. Motor performance (C) was impaired in a dose-dependent manner for CBZ and ESL expressed as time spent by the mouse on the rotarod, note the large rightwards shift in ESL impairment, indicating lower motor impairment. Symbols represent mean values of 12–15 animals per group.

(forelimb clonus moderate) or 2 (bilateral forelimb clonus with rearings high) during the first minute following current administration. ESL and CBZ exhibited a dose-dependent decrease in forelimb seizure scores (ED_{50} values of 15.9 and 9.5 mg/kg, respectively), with effects being significant at 50, 100 and 150 mg/kg for both anticonvulsants (Fig. 2B).

3.4. Rotarod test

The rotarod test was conducted in mice (n = 10 per group) trained to hold onto the rotarod apparatus until they maintain equilibrium up to 3 min while rotating at 15 rpm. The number of animals that drop off the rod was counted. CBZ and ESL were found to negatively affect motor coordination in a dose-dependent manner (Fig. 2C) albeit with TD_{50} values for CBZ (110.2, 68.7, 289.0 mg/kg) that were much lower than for ESL (313.7; 274.0, 353.0 mg/kg). The corresponding protective indexes (TD_{50}/ED_{50}) for CBZ (8.2 and 11.7, respectively of the MES and 6 Hz tests) were markedly lower than those for ESL (13.8 and 19.7, respectively of the MES and 6 Hz tests).

3.5. Pharmacodynamic/pharmacokinetic relationship

In the mouse, following the oral administration of 50 mg/kg ESL a 97% protection against MES-induced seizures was observed (Fig. 3). The levels of eslicarbazepine, the main active metabolite of ESL, in brain were 22 nmol/g total brain mass, which may be converted into an EC_{97} of 22 μM (in total brain volume). Since eslicarbazepine has a strong preference to stick to tissue material in a ratio of about 50:1 and that such tissue constitutes only 20% of the total brain volume, it is expected that the effective concentration of eslicarbazepine in the organic fraction of the brain will be higher than that measured in the whole brain volume. The calculated LogP of eslicarbazepine is 1.72, according to the software package ADMET Predictor (Simulations Plus, Inc), which corresponds to an octanol:water partitioning coefficient of 52.5. In the brain, it is also expected that eslicarbazepine will associate preferentially with organic tissue (lipids and proteins). After 72 h dehydration at 90 °C, the water fraction in the mouse brain was found to be approximately 80% of the brain mass (or volume) and therefore, in an average mouse brain of 358 ± 8 mg (n = 12), water comprises 281 ± 6 μl (n = 12), while the remaining 80 μl is comprised of cell

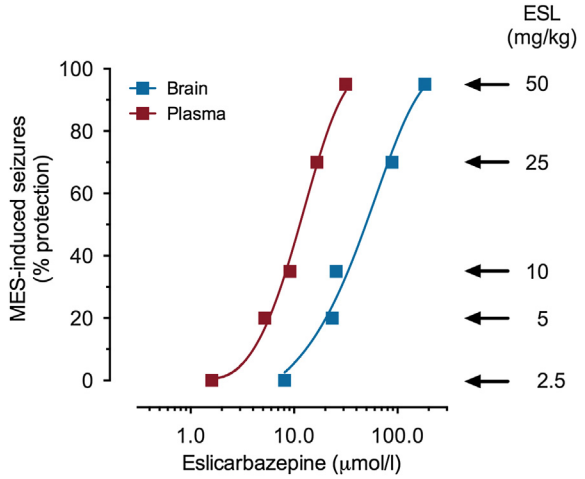

Fig. 3. Eslicarbazepine plasma and brain levels 60 min after the administration of ESL (2.5–50 mg/kg) and the effect on tonic convulsions on the mouse MES test. Symbols represent mean values of 5 animals per group.

structures, membranes, lipids, proteins, etc. As such, the concentration of eslicarbazepine in the organic fraction of the brain associated with effective 97% protection against MES-induced seizures should be 102 μM, which is 4.6 times higher than that measured directly in the total brain volume. However, eslicarbazepine does not show a strong affinity for binding (~30%) to non-specific proteins and may be preferentially associated to membranes, which constitute a smaller fraction of the dry weight of the brain. Assuming that bilipidic membranes constitute 10–12% of the total brain mass (Banay-Schwartz et al., 1992; McIlwain and Bachelard, 1985; Pratt et al., 1969), the corrected concentration of eslicarbazepine in the organic fraction of the brain was approximately 183 μM, which is 8.3 times higher than that measured directly in the total brain volume. As shown in Fig. 3, the brain concentration of eslicarbazepine was 5.8 times that in plasma. This was found to be independent of the dose of ESL administered, as evidenced by the parallelism of the eslicarbazepine concentrations in plasma and brain (Fig. 3). The concentration of eslicarbazepine in plasma associated with a 97% protection against MES-induced seizures was found to be 32 μM.

3.6. Identification of Na_V channel expressed in mouse N1E-115 neuroblastoma cells

To determine the suitability of N1E-115 cells to study neuronal VGSCs the expressed TTX sensitive Na_V channels were analysed using RT-PCR. The assays for NaV1.1, NaV1.2, NaV1.3 were specific for the target gene and showed no cross reactivity, while the assays for NaV1.6 and NaV1.7 showed some cross reactivity with cDNAs from different sodium channels (less than 100 times lower sensitivity). Relative gene expression in N1E-115 mouse neuroblastoma cells was calculated with ΔΔCt method (normalized to the housekeeping gene DNase I). The relative gene expressions as compared to NaV1.1 were as follows: NaV1.1: NaV1.2: NaV1.3: NaV1.6: NaV1.7 = 1.00: 1.31: 1.37: 2.17: 1.15, which is similar to that previously described (Niespodziany et al., 2013).

Further it was shown that N1E-115 cells did not metabolize oxcarbazepine, eslicarbazepine and R-licarbazepine (data not shown), which is in agreement with that reported by Araujo et al. (2004) in cultured hippocampal neurons.

3.7. Blockade of VGSC

To investigate the state dependence of VGSC block, eslicarbazepine and two classical anticonvulsants CBZ and OXC were tested on their ability to block VGSC at three different holding potentials (−60 mV, −80 mV and −100 mV) (Fig. 4A–C). The cells were depolarized for 10 ms to 0 mV every 6 s. For all compounds the IC_{50} values decreased at more positive holding potentials, as follows: holding potential −100 mV; IC_{50} (μM) for eslicarbazepine, CBZ and OXC was 15744.2, 822.9 and 1999.7, respectively; holding potential −80 mV; IC_{50} (μM) for eslicarbazepine, CBZ and OXC was 3105.9, 398.6 and 805.5, respectively; holding potential −60 mV; IC_{50} (μM) for eslicarbazepine, CBZ and OXC was 562.7, 108.7 and 172.8, respectively. CBZ and OXC showed a 7.5 or 11.6 times higher affinity to the VGSCs at a holding potential of −60 mV compared to −100 mV. For eslicarbazepine the absolute affinities were lower and, therefore, the IC_{50} values at very negative holding potentials could not be determined reliably. However, for eslicarbazepine the affinities at more positive potentials were found to be increased, indicating that all drugs tested preferentially interact with VGSCs in the inactivated state.

To analyse the mechanism by which eslicarbazepine interacts with VGSC, its characteristics were compared to LCM and the two classical anticonvulsants CBZ and OXC. First the current–voltage curves were recorded under control conditions and during perfusion of 250 μM of the drugs (Fig. 4C). When the membrane potential was depolarized to potentials more positive than −40 mV a fast inactivating inward current was observed. At potentials about −10 mV the peak current amplitude was maximal. The maximal peak current amplitude was reduced by eslicarbazepine (5.6%), CBZ (23.7%), LCM (20.1%) and OXC (24.4%) (Fig. 4D). The voltage dependence of activation gating was not significantly influenced by the tested drugs (Fig. 4E). The voltage dependence, the activation and the reversal potential which was close to the predicted Nernst equilibrium potential for sodium were similar for all tested compounds and consistent with the characteristics of fast inactivating VGSC (Fig. 4D–E).

3.8. Steady state fast inactivation of VGSC

To study the effects of the anticonvulsant drugs on the different inactivated states, first the steady state fast inactivation curves were recorded. For this, N1E-115 cells were clamped for 500 ms to potentials between −120 and −20 mV followed by a 10 ms test pulse to −10 mV (Fig. 5A). The short pre-pulse was selected to favour fast inactivation and to prevent slow inactivation of the VGSCs. Under control conditions the voltage of the half maximal steady state fast inactivation ($V_{0.5}$) was −68.7 ± 0.8 mV (n = 29). 250 μM CBZ and OXC shifted the $V_{0.5}$ value significantly ($P < 0.05$) to more hyperpolarized potentials (Fig. 5B and C). The $V_{0.5}$ values for eslicarbazepine and LCM were not significantly different compared to control conditions ($P > 0.05$). The slope (k) of the steady state fast inactivation curves were slightly increased (Table 1). To analyse the effect of the drugs on steady state fast-inactivated VGSCs in detail, the rate of recovery from fast inactivation was examined. N1E-115 neuroblastoma cells were clamped to −90 mV. A first test pulse of 10 ms to −10 mV was applied, followed by a 500 ms conditioning pulse to −10 mV to convert the voltage sensitive sodium channels into the fast-inactivated state. For the recovery of the channels a voltage pulse to −90 mV of varying duration was applied, followed by a second test pulse to −10 mV (10 ms) (Fig. 5D). The conditions of the voltage protocol were designed to avoid slow inactivation of the sodium channels. The peak current of the first test pulse represents the maximal current amplitude of VGSCs in the resting state. Therefore the amount of recovery can be calculated by dividing the current amplitude of the second test pulse by the first test pulse. When the duration of the recovery period was increased, the amplitude of the second test pulse increased (Fig. 5D and E). The time course of recovery could be fit with a biexponential function. Under control conditions, 78.7 ± 4.3% (n = 16) of the channels recovered from steady state fast inactivation with a time constant of 5.1 ± 0.5 ms. For eslicarbazepine and LCM, the time constant of the dominating fraction was not significantly ($P > 0.05$) different from control conditions, but for OXC ($P < 0.05$) it was about 5 times slower and for CBZ ($P < 0.05$) about 25 times slower (Table 1).

In another set of experiments, a series of 500 test pulses (20 ms to −10 mV) were delivered from a holding potential of −80 mV at 16.6 Hz. The available current in control and in the presence of drugs was calculated by dividing the peak current at any given pulse by the peak current in response to the initial pulse (pulse 1). The time course of current decay was fit with a biexponential function with a time independent current amplitude. The fast time constant was significantly faster for CBZ (0.29 ± 0.01 s) in comparison to control (0.93 ± 0.21 s), eslicarbazepine (0.57 ± 0.07 s) and LCM (0.57 ± 0.12 s). The slow time constant for CBZ (12.6 ± 2.6 s) was not significantly different from control (9.4 ± 0.7 s), but for eslicarbazepine (6.7 ± 0.8 s) and LCM (4.2 ± 0.3) significantly faster (Fig. 5F left). For better comparison of fast effects

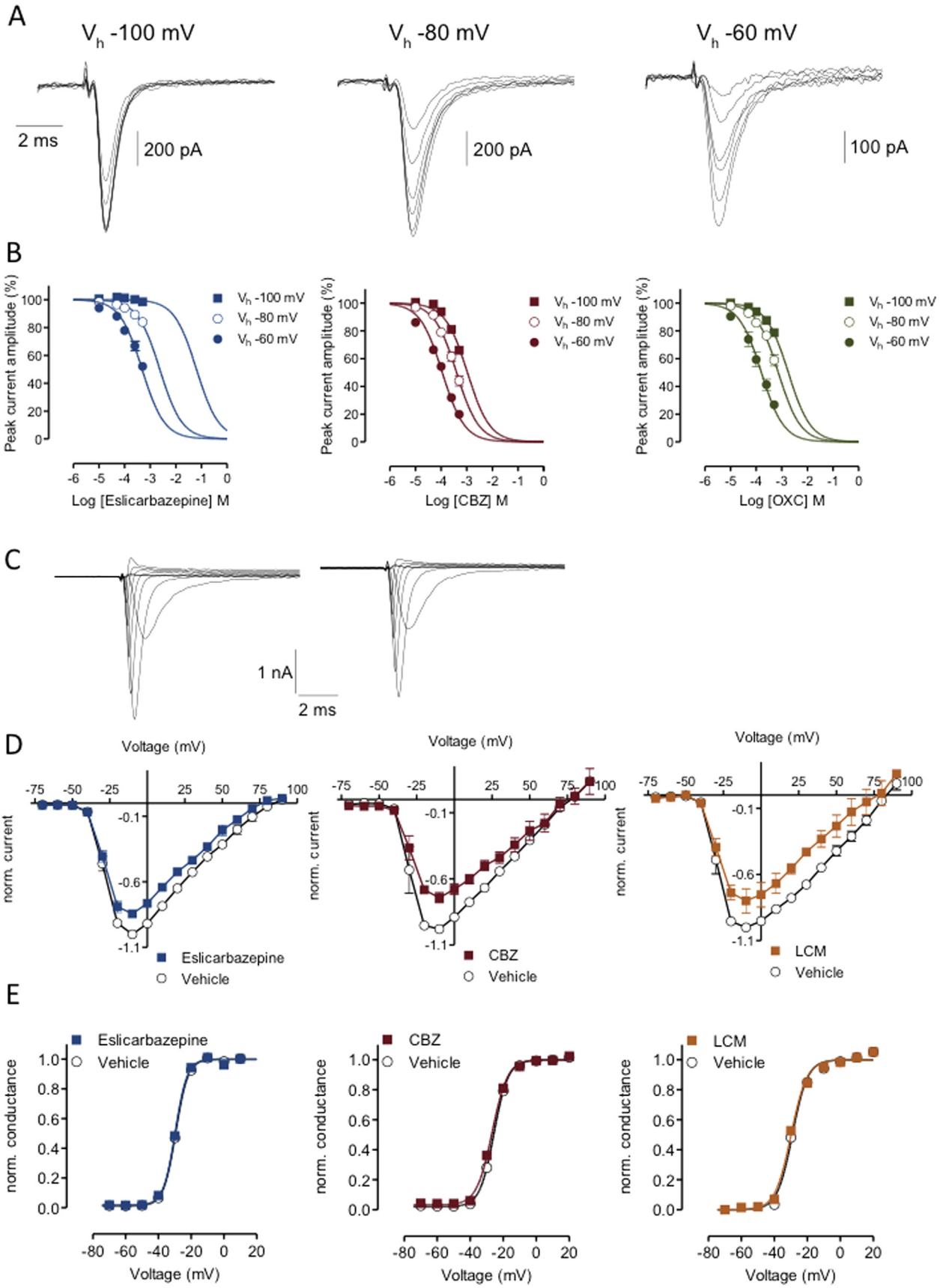

Fig. 4. The block of VGSC by eslicarbazepine and carbamazepine (CBZ) is voltage dependent. A) Representative current traces recorded from N1E-115 neuroblastoma cells. The cells were clamped to three different voltages (−100, −80 and −60 mV) and were depolarized to 0 mV every 6 s. Eslicarbazepine, carbamazepine (CBZ) and oxcarbazepine (OXC) were tested in 5 concentrations (10, 50, 100, 250 and 500 μM), perfused until the steady state was reached, and steady state currents were superimposed for control conditions. B) For

first 30 pulses are shown (right). For this plot remaining (time independent) current amplitudes were subtracted before normalization to the first pulse. CBZ markedly reduced current amplitude compared with controls by the third pulse in the train, but currents in the presence of eslicarbazepine or LCM were almost superimposable with controls (Fig. 5F right). It is interesting that eslicarbazepine and LCM began to show some degree of use-dependent block, with a distinct latency, only after approximately 10–11 test pulses (Fig. 5F, right arrow). However, even by the last of the 30 pulses delivered, the peak current available was still not significantly different from control conditions. In contrast, by the 30th test pulse in the train the available peak current in the presence of CBZ was significantly reduced when compared with control.

3.9. Slow inactivation of VGSC

VGSCs expressed in N1E-115 mouse neuroblastoma cells enter a slow inactivation state after prolonged periods of depolarization (Matsuki et al., 1984; Quandt, 1988). To determine the time necessary for VGSC to change the conformation to the slow inactivation state, a depolarizing pulse of increasing durations (0, 10, 20 and 30 s, at −20 mV) was used. Before and after this pulse, a test pulse of 10 ms to −10 mV was applied. To exclude any contamination by fast-inactivated channels, the cells were hyperpolarized for 1.5 s to −90 mV between the long depolarizing pulse and the second test pulse (Fig. 6A). This pulse should be sufficient to recover all steady state fast-inactivated channels to the resting state. To calculate the amount of steady slow inactivation, the peak current amplitude of the second test pulse was divided by the peak current amplitude of the first test pulse. This ratio was plotted versus the time of the long depolarizing pulse and fit with a monoexponential function (Fig. 6B). Under control conditions the time constant (τ) for entering the slow inactivated state was 18.0 ± 1.6 s. For CBZ and OXC (250 μM) the entry was only slightly faster (13.0 ± 1.7 s and 12.6 ± 0.9 s, respectively), while it was more than two times faster for eslicarbazepine (7.3 ± 0.9 s; $P < 0.05$) and LCM (5.6 ± 0.9 s; $P < 0.01$) compared to control conditions. Besides the kinetic of entering the slow inactivated state, also the remaining current amplitudes were affected by the perfused test drugs. After a depolarization of 30 s under control conditions, 64.3 ± 1.2% ($n = 18$) of the channels were available and not in the non-conducting slow inactivated state. For CBZ and OXC the number of available channels was slightly larger than under control conditions. This may be caused by a faster recovery from slow inactivation (compare Table 1) during the hyperpolarizing pulse before the second test pulse (Fig. 6A). The observed relative current amplitude compared to control conditions was similarly reduced ($P < 0.05$) by eslicarbazepine (59.2 ± 3.5%, $n = 6$) and LCM (55.4 ± 3.2% ($n = 6$) (Fig. 6B).

To investigate the effect of the anticonvulsant drugs on the voltage dependence of steady state slow inactivation, neuroblastoma cells in the whole-cell configuration were held at −80 mV, stepped to pre-pulse potentials between −120 mV and +50 mV (10 mV increments, 5 s duration) and hyperpolarized to −80 mV for 1 s to convert fast-inactivated channels in the resting state. To investigate the amount of available channels, a test pulse to −10 mV (10 ms duration) was applied (Fig. 6C). The peak current amplitudes of the test pulse were plotted against the potential of the pre-pulse and fitted with a Boltzmann function including a voltage independent rest (Fig. 6D). Data recorded under control conditions or during perfusion of 250 μM of the tested drugs could be well fitted except for OXC. In the range between −80 mV and −50 mV, the peak current was smaller then predicted by the fit. One explanation for this effect could be the prolonged recovery time of the VGSC from the fast-inactivated state during OXC perfusion (Table 1). To explore this hypothesis the same voltage protocol was used, but the duration of the hyperpolarizing pulse between the pre-pulse and the test pulse was increased from 1.0 s to 1.5 s. Under these conditions the data over the entire voltage range could be well fit with a Boltzmann function, but the amount of the voltage-dependent fraction decreased and a larger voltage independent rest remained (Fig. 6F). The $V_{0.5}$ was −9.7 ± 4.3 mV ($n = 6$) and almost identical to control conditions ($V_{0.5}$ −10.2 ± 5.7 mV, $n = 4$). Under these experimental conditions the time constants for recovery from fast and slow inactivation differ only by a factor of 31.3 in the presence of 250 μM OXC (Table 1). For CBZ this factor is even lower (8.3). Therefore a similar effect of the two drugs on the slow inactivation curve would have been expected, but as CBZ does not significantly influence the voltage dependence of the steady state slow inactivation, the slow inactivation curve could well described with a Boltzmann function (Fig. 6D). For all other drugs tested, significant shifts of the $V_{0.5}$ values were observed (Table 1). The largest shift was observed for 250 μM LCM (−53.3 mV), while the shift for eslicarbazepine was less pronounced (−31.2 mV). In parallel, the slope (k) of the slow inactivation curves was increased for all tested compounds, even for CBZ, compared to control conditions (Table 1).

The recovery from the slow inactivated state was also analysed. The VGSC of N1E-115 cells were inactivated by a long (10 s) pulse to −20 mV. To switch fast-inactivated channels into a resting state, the cells were clamped to −80 mV for 1.5 s before applying test pulses (10 ms, −10 mV) every 1.5 s (Fig. 7A). The peak current amplitudes represent the amount of available, not inactivated, channels. The time course of recovery from the slow inactivated state could be fit with a monoexponential function (Fig. 7B). As previously described (Errington et al., 2008), the half-life recovery (τ) for LCM (250 μM, $n = 4$) was not significantly different when compared to control conditions ($n = 22$). Also for eslicarbazepine the time course of recovery was not significantly influenced, whereas CBZ and OXC significantly decreased the time necessary for the slowly inactivated VGSC to become available for activation ($P < 0.05$), as depicted in Table 1.

To compare the tonic affinity of the drugs to slow inactivated channels in comparison to VGSC in the resting state, the IC_{50} values for both states were determined. The voltage protocol contained two test pulses (10 ms, −10 mV). The first test pulse was applied after the neuroblastoma cells were held at −90 mV for at least 180 s and was used to determine the IC_{50} in the resting state. The second test pulse – that was used to determine the IC_{50} at the slow inactivated state – was applied after cells were depolarized for 10 s at −20 mV and fast-inactivated VGSC have been converted to the resting state by a 1.5 s pulse to −80 mV (Fig. 6G). Concentrations of 10, 100 and 1000 μM were tested (Fig. 6H). The affinity for all tested

each holding potential concentration response curves were generated. The peak current amplitudes were normalized to the peak current amplitude under control conditions and plotted versus the perfused concentration. C) Representative recordings of VGSC expressed in N1E-115 neuroblastoma cells. Cells were clamped to −100 mV for 500 ms before voltages between −70 mV and +90 mV were applied ($V_{hold} = -80$ mV). Left: control conditions, right: during perfusion of 250 μM eslicarbazepine after steady state was reached. D) Current–voltage curves were generated by plotting the peak current amplitude versus the applied voltage in the presence of vehicle or test drugs (250 μM). All data were normalized to the maximal current amplitude observed under control conditions. E) Activation curves were derived from the current–voltage curves in the presence of vehicle or test drugs (250 μM). Data were fit with a sigmoidal two-parameter equation and each activation curve was normalized to its maximum conductance and fit with a Boltzmann function.

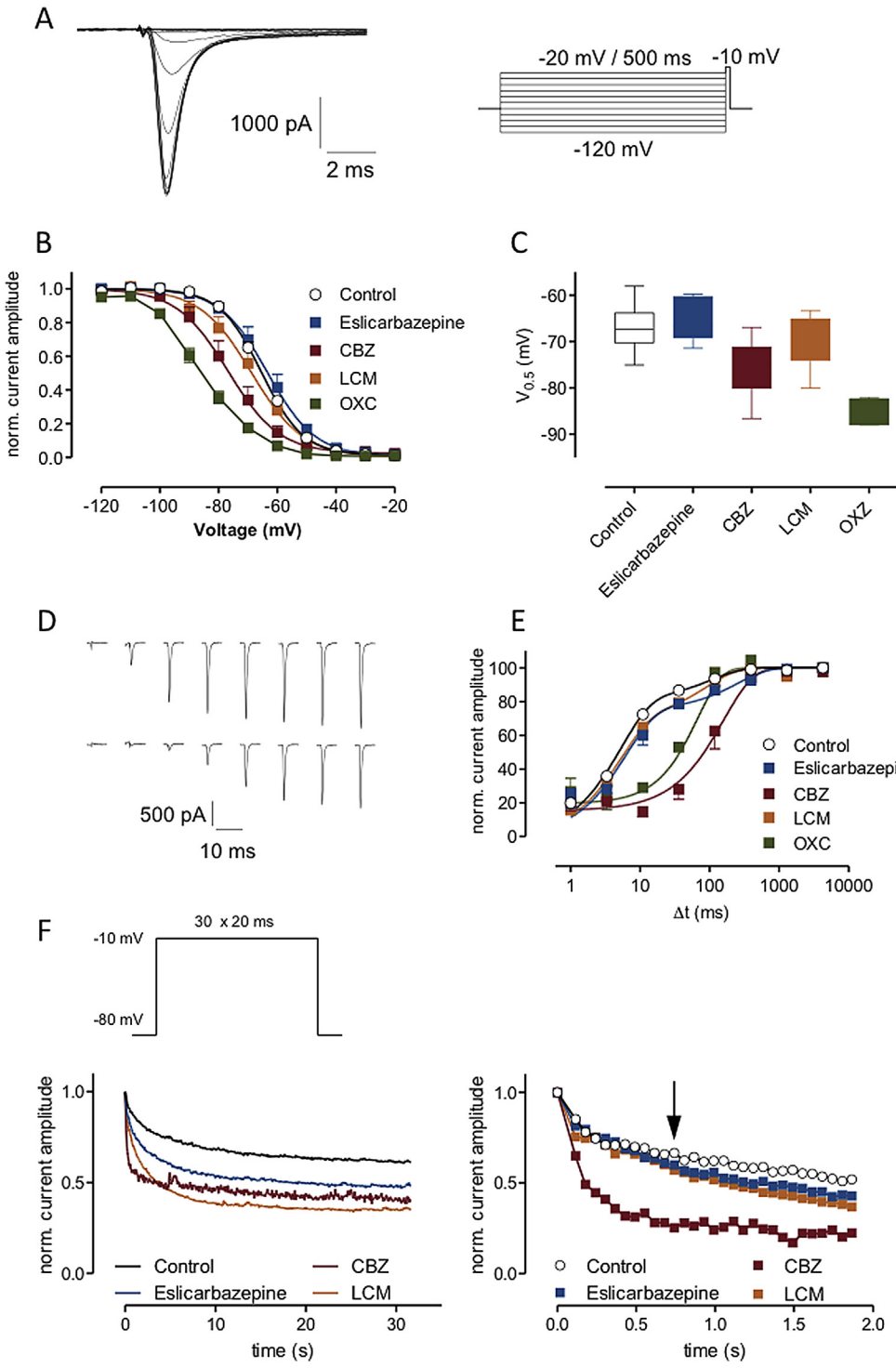

Fig. 5. Eslicarbazepine and lacosamide (LCM) do only slightly influence fast inactivation. A) Representative tail currents of VGSC under control conditions (left) or during perfusion of 250 μM eslicarbazepine (right). N1E-115 cells were depolarized to potentials between −120 mV and −20 mV for 500 ms before a test pulse to −10 mV was applied. Only currents recorded during this test pulse are shown. B) Inactivation curves were constructed in the presence of vehicle or test drugs (250 μM). All current amplitudes were normalized to the maximal current amplitude and plotted versus the voltage of the pre-pulse. Each curve was fit with a Boltzmann function. C) Mean $V_{0.5}$ (voltage of the half maximal steady state fast inactivation) values were collected from all analysed cells and averaged, visualizing the shift of the voltage dependence of fast inactivation by the tested drugs. D) Recovery of VGSC from the fast-inactivated state. VGSC were converted to the fast-inactivated state by a 500 ms pulse to −10 mV. This pulse was followed by a pulse to −90 mV for increasing duration. Before and after these pulses a test pulse to −10 mV (duration 10 ms) was applied. The peak-current amplitudes of the second test pulse were normalized to the peak current amplitude of the test pulse before the inactivating long pulse. Top: control conditions, Bottom: during perfusion of 250 μM carbamazepine E) These normalized current amplitudes were plotted versus the duration of the pulse before the second test pulse in the presence of vehicle or test drugs (250 μM). Data were fit with a biexponential function. F) Plot summarizing the frequency-dependent decrement in peak current amplitude (mean value from replicated experiments, for clarity error, bars are not shown, values are quoted in text) Left: Voltage protocol and Time course of peak current amplitudes for 500 pulses (16.6 Hz). Data were normalized to the amplitude of the first pulse. For better comparison of fast effects first 30 pulses are shown (right). For this plot remaining current amplitudes were subtracted before normalization to the first pulse. CBZ, but not eslicarbazepine and LCM caused fast effects upon current amplitudes. After only 5 pulses, 250 μM CBZ produced significantly more attenuation of current than under control conditions. In contrast, 250 μM eslicarbazepine and 250 μM LCM exerted no significant ($P > 0.05$) frequency-dependent facilitation of block even after 30 pulses, although a slow reduction in the peak current was observed beginning after approximately 10–11 pulses (arrow).

Table 1
Parameters of fast and slow inactivation and of time course of recovery from fast and slow inactivation.

Parameters of fast and slow inactivation				
	Fast inactivation		Slow inactivation	
	$V_{0.5}$ (mV)	k	$V_{0.5}$ (mV)	k
Control	−68.66 ± 0.84 (n = 29)	6.77 ± 0.1 4 (n = 29)	−16.21 ± 1.21 (n = 13)	13.60 ± 0.34 (n = 13)
Eslicarbazepine	−65.12 ± 2.15 (n = 5)	7.41 ± 0.16 (n = 5)	−47.37 ± 3.15 (n = 6)	23.35 ± 1.62 (n = 6)
CBZ	−75.66 ± 2.66 (n = 6)	7.82 ± 0.73 (n = 6)	−20.84 ± 1.97 (n = 4)	19.21 ± 2.08 (n = 4)
OXC	−85.24 ± 1.54 (n = 4)	9.08 ± 0.31 (n = 4)	−44.27 ± 1.92 (n = 4)	23.42 ± 0.97 (n = 4)
LCM	−73.42 ± 2.72 (n = 5)	8.67 ± 0.48 (n = 5)	−69.49 ± 1.26 (n = 5)	15.75 ± 0.68 (n = 5)

Parameters of time course of recovery from fast and slow inactivation			
	Fast inactivation[a]		Slow inactivation
	τ_1 (ms)/amplitude (%)	τ_2 (ms)/amplitude (%)	τ (s)
Control	5.06 ± 0.49/78.73 ± 4.30 (n = 16)	203.65 ± 40.27/21.27 ± 4.30 (n = 16)	3.61 ± 0.27 (n = 22)
Eslicarbazepine	7.49 ± 0.84*/78.31 ± 3.81 (n = 3)	347.17 ± 56.52/21.69 ± 3.81 (n = 3)	3.42 ± 0.46 (n = 5)
CBZ	132.83 ± 40.09*/92.41 ± 3.13 (n = 3)	1165.55 ± 939.55/7.59 ± 3.13 (n = 3)	1.31 ± 0.07 (n = 4)
OXC	34.04 ± 2.51*/93.02 ± 3.42 (n = 3)	1457.05 ± 142.87*/6.98 ± 3.42 (n = 3)	1.13 ± 0.09 (n = 5)
LCM	4.98 ± 0.63/67.03 ± 2.86 (n = 6)	78.52 ± 5.17*/32.97 ± 2.86 (n = 6)	4.27 ± 0.76 (n = 4)

Values are means ± SEM from the indicated number of independent determinations. Significantly different from control values (*P < 0.05).
[a] Values were obtained from a fit to the averaged data from the indicated number of independent determinations.

drugs was higher if more channels were in the slow inactivated state than in the resting state. The affinity to VGSC in the rested state was highest for CBZ (459.7 μM) and lowest for eslicarbazepine (3301.6 μM). For LCM, the affinity increased 10.4 times after channels have been slowly inactivated by a long depolarization (resting state = 1889.2 μM; slow inactivated state = 181.8 μM). For eslicarbazepine a similar effect was observed, but the IC_{50} differed only by a factor of 5 (resting state = 3301.6 μM; slow inactivated state = 559.3 μM), and for CBZ (resting state = 459.7 μM; slow inactivated state = 263.1 μM) and OXC (resting state = 776.1 μM; slow inactivated state = 424.3 μM) the difference was even lower, the IC_{50} under conditions of slow inactivation was only halved compared to the resting state.

4. Discussion

N1E-115 mouse neuroblastoma cells express a variety of endogenous neuronal TTX-sensitive Na_V sodium channels (NaV1.1, NaV1.2, NaV1.3, NaV1.6 and NaV1.7), which make the cells useful to test anticonvulsant drugs. The results presented here show that eslicarbazepine acted as a blocker for VGSCs in N1E-115 cells, but with lower affinities than known anticonvulsant drugs like CBZ, OXC and LCM. The IC_{50} values of all tested drugs were voltage dependent with lower values at more depolarized potentials. Inhibition of VGSC by this type of drugs is usually increased by depolarization because they bind preferentially to the inactivated state of the channel (Catterall, 1999). The voltage dependence was especially profound for eslicarbazepine and may indicate that this compound preferably interacts with inactivated VGSC. The finding that neither the voltage dependence of the current–voltage curves, nor the voltage dependence of activation was significantly affected by perfusing 250 μM of eslicarbazepine further supported this proposed mechanism of action. At this level of exposure, eslicarbazepine markedly attenuated epileptiform activity in mouse hippocampus slices following exposure to Mg^{2+}-free/4-AP and was associated with prevention of the development of seizures induced in the MES and the 6-Hz psychomotor tests.

For VGSC several different modes of inactivation have been described. At least two different inactivated states can be distinguished by the entry time. Within milliseconds of depolarization the channels enter the fast-inactivated state while it lasts up to several seconds for slow inactivation. For analysing effects of the fast-inactivated state only short (500 ms) depolarizations were applied. Under these conditions, only CBZ and OXC significantly shifted the voltage dependence of inactivation to more negative potentials, indicating an increasing affinity to VGSC with increasing amounts of fast inactivation. Also recovery from fast inactivation was slowed only by CBZ and OXC, but not by LCM and eslicarbazepine.

During long (several seconds) depolarizations, VGSC convert to the non-conducting slow inactivated state. This transition into the slow inactivated state was not affected by CBZ or OXC, but for eslicarbazepine it was twice and for LCM four times faster than under control conditions. Also the voltage dependence of slow inactivation was shifted to more hyperpolarized potentials, indicating an increased affinity to slow inactivated VGSC. This result was also confirmed by the determination and comparison of the IC_{50} values under resting and steady state slow inactivated conditions. Recovery from the slow inactivated state was not significantly different in the presence of eslicarbazepine or LCM, while it was faster during perfusion of CBZ and OXC. In practice due to experimental limitations it is difficult to select conditions at which fast or slow inactivation can be observed separately: the tested compounds change the voltage dependence and time courses of ON and OFF rates. This leads to an overlap of these parameters that are well separated under control conditions. Therefore a contamination by VGSC in other inactivation states cannot be excluded. Due to the delayed recovery from fast inactivation and an accelerated recovery from slow inactivation in the presence of OXC it was not possible to record the voltage dependence of slow inactivation without contamination by fast-inactivated channels or a large fraction of channels that already recovered from slow inactivation under the experimental conditions chosen. A more suitable pulse protocol might be designed based on analysis of the voltage dependence of recovery from fast inactivation and the time course of entering the slow inactivated state. Also the IC_{50} values determined for resting state and slow inactivated state are probably underestimated for both states. A more negative holding potential would have resulted in a higher IC_{50} for the resting state, while a prolonged depolarizing pulse exceeding the time constant for the entry into the slow inactivated state would have resulted in a lower IC_{50} for the slow inactivated state.

Our results are in agreement with those previously reported on the characterization of the effects of LCM upon fast and slow

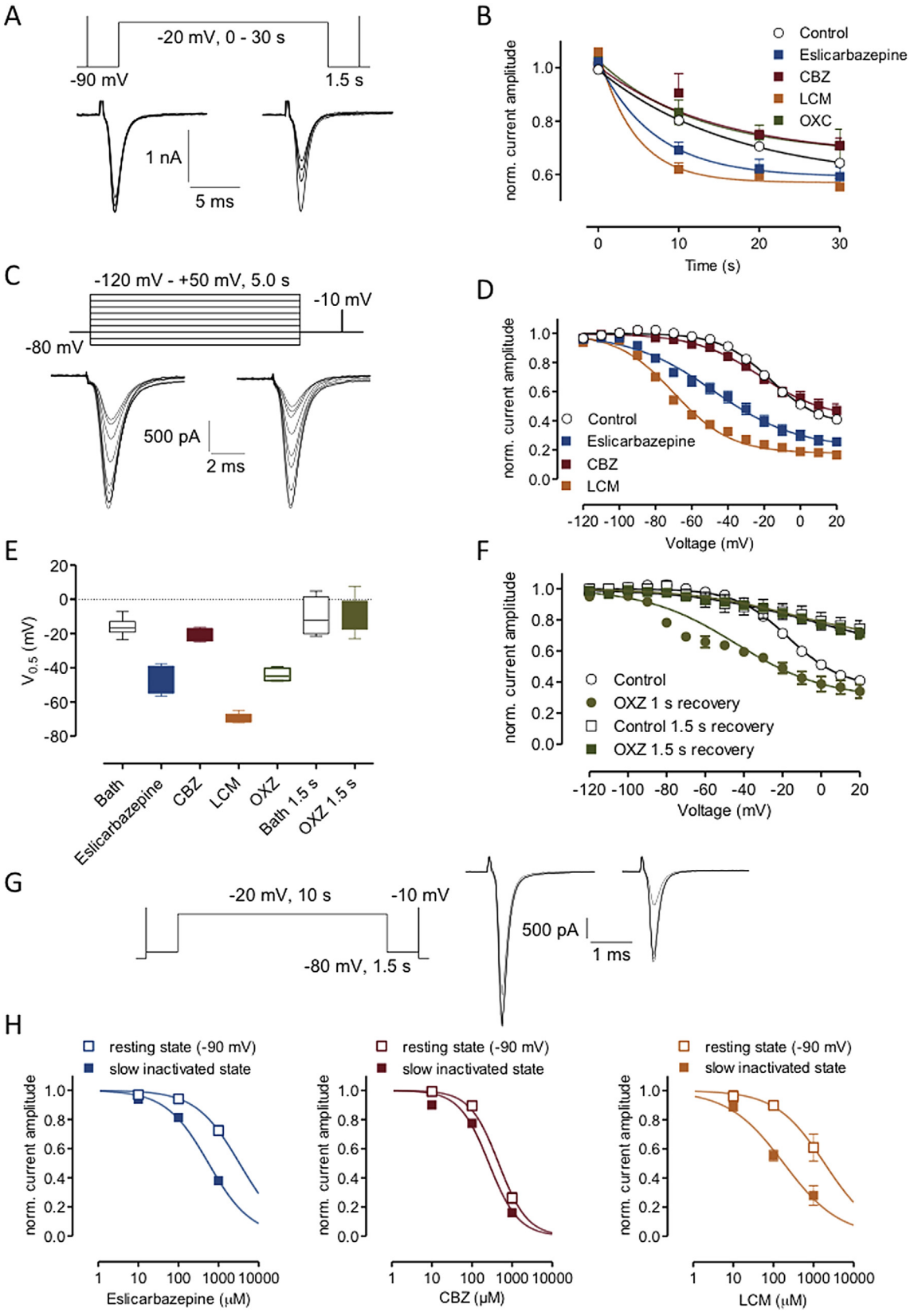

Fig. 6. The entry into the slow inactivated state as well as its voltage dependence is influenced by eslicarbazepine and lacosamide (LCM). A) N1E-115 neuroblastoma cells were depolarized for 0, 10, 20 or 30 s to −20 mV to enhance slow inactivation. To convert fast-inactivated channels into the resting state a pulse to −90 mV (duration 1.5 s) was applied. Before and after this pulse test pulses to −10 mV (10 ms duration) were applied to analyse the amount of available VGSC. Representative current traces for the first (left) and the second (right) test pulse are superimposed during perfusion of 250 μM eslicarbazepine. B) Peak current amplitudes of the second test pulse were normalized to the peak current amplitude of the second test pulse and plot versus the duration of the depolarizing pulse in the presence of vehicle or test drugs (250 μM). Data were fit with a monoexponential function. C) Slow inactivation curves were recorded using voltage pulses between −120 and +50 mV (5 s duration) followed by a pulse to −80 mV (duration 1 s) and a test pulse

inactivated VGSC (Errington et al., 2008). This was the first description of an anticonvulsant drug with a low affinity to VGSC in the fast-inactivated state, but a significantly increased affinity to channels in the slow inactivated state. However, it should be underscored that the effects upon slow inactivation may change according the Na_v subunits involved (Niespodziany et al., 2013). In a next step single isoforms of the VGSC should be characterized. This was a new mechanism of action that could selectively affect sodium channels at a higher degree of inactivation caused by prolonged depolarization or an increased frequency of action potentials. Our results indicate that eslicarbazepine may act via a similar mechanism, what might also explain why eslicarbazepine shows a favourable safety profile compared to the classical anticonvulsant drugs like CBZ (Gil-Nagel et al., 2013) and OXC (Milovan et al., 2010; Nunes et al., 2013), which preferably interact with fast-inactivated channels.

Fast inactivation of Na^+ channels is thought to contribute to action potential termination and regulation of the refractory period (McCollum et al., 2003). Slow inactivation, on the other hand, may play a role in regulating excitability, such as by modulating burst discharges. In fact, this modulation appears to be complex since slow inactivation not only depends on resting potential but also on previous history of action potential firing (Ulbricht, 2005). Slow inactivation occurs on a much slower time scale of seconds and is a more complex process involving amino acids lining the S6 segments (Chen et al., 2006; O'Reilly et al., 2001). Mechanistically, fast inactivation has been shown to involve the short intracellular loop between domains III and IV (McPhee et al., 1994; West et al., 1992) although additionally sites within IV S6 (McPhee et al., 1994) and within the S4–S5 loop of both domains III and IV have also been implicated (McPhee et al., 1998). Slow inactivation is thought to contribute to overall membrane excitability by increasing action potential thresholds, thereby limiting action potential burst durations and importantly, limiting the propagation of action potentials within dendrites. Therefore, modulation of Na^+ channel availability through enhancement of slow inactivation by either endogenous (Chen et al., 2006) or pharmacological methods could have significant effects on membrane excitability, particularly during epileptic seizures (Rogawski and Loscher, 2004). Amino acids located in the P loop form an outer ring of charges were found to be associated with slow inactivation (Xiong et al., 2003). Our data have shown that CBZ does not significantly change any characteristics of slow inactivation. Phenytoin, CBZ and lamotrigine were demonstrated to block the pore of VGSC by binding via aromatic–aromatic interaction to the side chain of a tyrosine and phenylalanine located in the IV S6 helix (Lipkind and Fozzard, 2010). As eslicarbazepine and LCM may block the channel pore almost only during slow inactivation, it is likely that they may bind at a different position to the channel protein.

CBZ induced significant concentration-dependent inhibition of epileptiform activity evoked by exposure to Mg^{2+}-free/4-AP bathing medium. These effects were for the main part associated with an increase in neuronal input resistance, suppression of spontaneous synaptic transmission and inhibition of action potential firing. Eslicarbazepine induced a suppression of epileptiform activity in a concentration-dependent manner with no significant

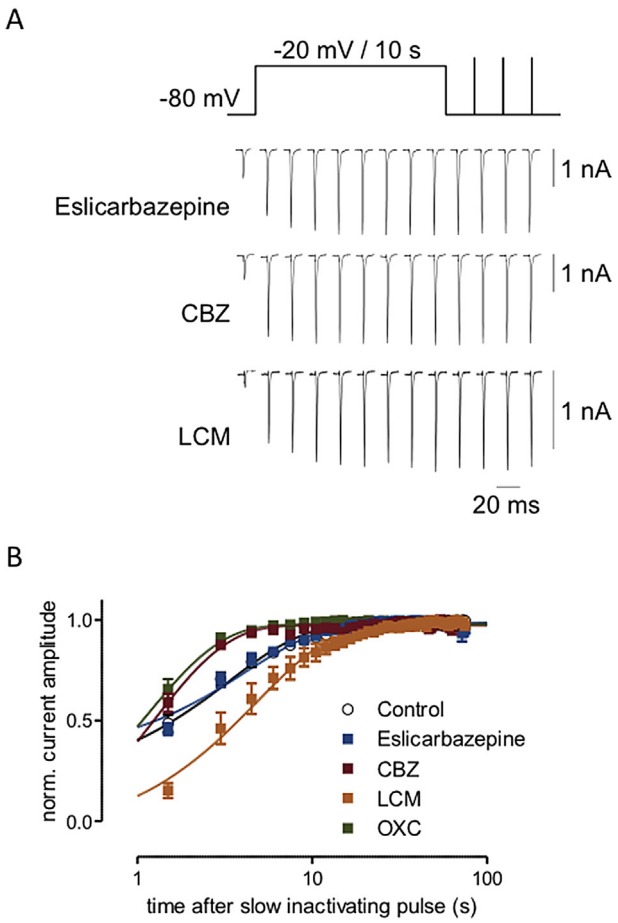

Fig. 7. Eslicarbazepine does not influence the recovery from slow inactivation. A) To analyse the recovery from steady state slow inactivation N1E-115 cells clamped to −80 mV. VGSC were inactivated by a 10 s pulse to −20 mV, followed by a train of test pulses (−10 mV, 10 ms duration) separated by 1.5 s where the cells were clamped to −80 mV. Representative traces of every second test pulse are shown. B) Peak current amplitudes were normalized to the maximal peak current amplitude and plotted versus the time after the long slow inactivating pulse. Data were fit with a mono-exponential function.

effect on neuronal input resistance. The preferential binding to slow inactivated states for eslicarbazepine most likely reflects its less marked reduction upon spontaneous firing rate and in Mg^{2+}-free/4-AP bathing medium. Similar findings were reported for LCM using this experimental model (Lees et al., 2006). Under *in vivo* experimental conditions in two different models of acute seizures in the mouse (the MES and the 6-Hz psychomotor tests), both ESL and CBZ exerted dose dependent anticonvulsant properties with similar magnitude. However, the corresponding protective indexes for CBZ were markedly lower than those for ESL. The tested concentrations and IC_{50}'s of eslicarbazepine in *in vitro* experiments seem to be high when compared to those of clinical relevance. In human clinical use, oral administration of ESL at 1200 mg once daily results in approximate peak plasma concentrations of 90 μM.

to −10 mV (10 ms duration) to analyse the amount of available VGSC. This protocol was run under control conditions (left) and during perfusion of 250 μM eslicarbazepine (right). D) To generate slow inactivation curves, all peak current amplitudes were normalized to the maximal current amplitude and fit with a modified Boltzmann function. E) Summary of $V_{0.5}$ (voltage of the half maximal steady state slow inactivation). F) Slow inactivation curves under control conditions and during perfusion of 250 μM OXC using 1 or 1.5 s (−80 mV) for recovery of fast-inactivated channels. Affinity to VGSC after steady state slow inactivation is more increased by eslicarbazepine and lacosamide (LCM) compared to carbamazepine (CBZ). G) Concentration response curves of eslicarbazepine for VGSC in the resting and in the slow inactivated state were analysed with the same voltage protocol. The test pulse before the inactivating pulse (−20 mV for 10 s) was used to determine the IC_{50} in the resting state, while the second test pulse was used to analyse the affinity of the channels after slow inactivation. Representative current recordings for the resting state (left) and for slowly inactivated VGSC (right) are shown. H) After perfusing the test item for 180 s with the peak current amplitude under control conditions. Data were fit with a sigmoidal two-parameter function.

The *in vitro* studies described above on the interaction of VGSCs were conducted at higher concentrations (250–300 μM). However, the concentrations used in this study may be justified for the following reasons. Since eslicarbazepine has a strong preference to stick to tissue material in a ratio of about 50:1 and that such tissue constitutes only 20% of the total brain volume, it is expected that the effective concentration of eslicarbazepine in the organic fraction of the brain are higher than that measured in the whole brain volume. Eslicarbazepine did not show a strong affinity for binding (~30%) to non-specific proteins (Bialer and Soares-da-Silva, 2012) and may preferentially associated to membranes, which constitute a smaller fraction (10%–12%) of the dry weight of the brain (Banay-Schwartz et al., 1992; McIlwain and Bachelard, 1985; Pratt et al., 1969). The corrected EC_{97} values in the organic fraction (102 μM) or the lipid fraction (183 μM) of the brain are close to IC_{50} values obtained in patch-clamp experiments measuring the effects of eslicarbazepine upon voltage-gated sodium currents, namely under depolarizing conditions at less negative holding potentials (Hebeisen et al., 2011). The corresponding mouse plasma levels (Fig. 3) are within the range to those observed in patients with POS (Perucca et al., 2011) or healthy volunteers taking ESL at therapeutic doses (Elger et al., 2013). This is in line with the fact that eslicarbazepine does not distribute well within the aqueous phases such as CSF (Nunes et al., 2013) or water in brain. This might explain the apparent discrepancies observed on the effective concentrations between *in vivo* and *in vitro* experiments. It is worthwhile to underscore that CSF C_{max} eslicarbazepine attained levels of 30 μM while using 1200 mg QD ESL (Nunes et al., 2013). Assuming that eslicarbazepine therapeutic level in the CNS tissue is in equilibrium in that in the CSF, which is most probably not the case because of the high lipid:water partition coefficient (50:1) described above, then the *in vitro* experiments performed with 300 μM were 10 times higher the putative therapeutic level. The study establishing that LCM promotes the slow inactivation of VGSC was conducted at concentrations ranging from 32 to 320 μM, the most relevant results obtained at 100 μM LCM (Errington et al., 2008). In human clinical use, oral administration of LCM at 600 mg twice daily results in approximate peak plasma concentrations of (14.5 μg/mL or 58 μM) (Ben-Menachem et al., 2007). Since LCM protein binding corresponds to approximately 15% (Doty et al., 2007), then the systemic peak plasma concentrations of 58 μM LCM falls to 9 μM LCM free drug, which is 10 times lower the putative therapeutic level used by Errington et al. (2008).

A rational approach to AED polytherapy for patients that do not achieve seizure control with a single AED is a matter of considerable debate. AED combinations with the same mechanism of action may theoretically be less optimal than targeting different mechanisms of action (Brodie and Sills, 2011; Kwan and Brodie, 2006). However, this may be difficult to implement, since many AEDs exert multiple mechanisms (Rogawski and Loscher, 2004; Stafstrom, 2010). Another unresolved issue is whether AEDs with different mechanisms of action are more likely to interact synergistically than AEDs with similar or differing mechanisms (Kwan and Brodie, 2006; Stafstrom, 2010). Combinations of AEDs with similar mechanisms of action may cause exaggerated additive/supra-additive adverse effects; combinations of AEDs that target VGSC are regarded as offering only additive improvements in efficacy and frequently supra-additive enhancement of neurotoxicity (Brodie and Sills, 2011; Kwan and Brodie, 2006). While most VGSC blockers used in the treatment of epileptic seizures interfere with the fast inactivation pathway, the results shown here indicate that eslicarbazepine and LCM selectively influences slow inactivation, which fits well the view that they can be usefully combined with VGSC blockers that act on fast inactivation. In fact, the efficacy of adjunctive ESL, which results in exposure to largely eslicarbazepine, in reducing the frequency of partial-onset seizures in adults receiving CBZ or another AED was similar (Halasz et al., 2010; Hufnagel et al., 2013). In a post-hoc exploratory analysis, adjunctive LCM demonstrated significant seizure reduction over placebo regardless of the inclusion of 'traditional' sodium channel blockers in the concomitant AED regimen (Sake et al., 2010). A pooled ESL analysis showed that although the incidence of treatment emergent adverse events (TEAEs) was higher in patients treated with CBZ than in patients not treated with CBZ, the incidence of any TEAE in the ESL groups was generally comparable in both subpopulations (Gil-Nagel et al., 2013). However, other distinctive properties of eslicarbazepine over CBZ also include 10- to 60-fold higher potency for the blockade of low and high affinity $hCa_v3.2$ inward currents (Brady et al., 2011), being devoid of effects upon $hCa_v2.1$ inward currents whereas CBZ inhibited $hCa_v2.1$ calcium peak currents (Bonifacio et al., 2012).

In conclusion, eslicarbazepine may not share with CBZ and OXC the ability to alter fast inactivation of VGSC. Both eslicarbazepine and LCM reduce VGSC availability through enhancement of slow inactivation, but LCM demonstrated higher interaction with VGSC in the resting state and with fast inactivation gating. The apparent discrepancies observed on the effective concentrations between *in vivo* and *in vitro* experiments may be explained by the physicochemical properties of eslicarbazepine, namely its lipophilicity.

Disclosure

Simon Hebeisen was an employee B'SYS GmbH Analytics at the time of the study. B'SYS GmbH Analytics, Prof. David Spanswick, Dr. Andrew Whyment and Neurosolutions Ltd have received grants from BIAL – Portela & C[a], S.A. Nuno Pires, Ana I. Loureiro, Maria João Bonifácio, Nuno Palma and Patricio Soares-da-Silva were employees of BIAL – Portela & C[a] S.A. at the time of the study.

Acknowledgements

This study was supported by BIAL – Portela & C[a], S.A.. We thank Michel Dolder for his excellent technical assistance.

References

Almeida, L., Soares-da-Silva, P., 2007. Eslicarbazepine acetate (BIA 2-093). Neurotherapeutics 4, 88–96.

Araujo, I.M., Ambrosio, A.F., Leal, E.C., Verdasca, M.J., Malva, J.O., Soares-da-Silva, P., Carvalho, A.P., Carvalho, C.M., 2004. Neurotoxicity induced by antiepileptic drugs in cultured hippocampal neurons: a comparative study between carbamazepine, oxcarbazepine, and two new putative antiepileptic drugs, BIA 2-024 and BIA 2-093. Epilepsia 45, 1498–1505.

Banay-Schwartz, M., Kenessey, A., DeGuzman, T., Lajtha, A., Palkovits, M., 1992. Protein content of various regions of rat and adult aging human brain. Age 15, 51–54.

Ben-Menachem, E., Biton, V., Jatuzis, D., Abou-Khalil, B., Doty, P., Rudd, G.D., 2007. Efficacy and safety of oral lacosamide as adjunctive therapy in adults with partial-onset seizures. Epilepsia 48, 1308–1317.

Bialer, M., Soares-da-Silva, P., 2012. Pharmacokinetics and drug interactions of eslicarbazepine acetate. Epilepsia 53, 935–946.

Bonifacio, M.J., Brady, K., Hebeisen, S., Soares-da-Silva, P., 2012. Effects of eslicarbazepine, R-licarbazepine and oxcarbazepine on ion transmission through $Ca_v2.1$ and $Ca_v3.2$ channels. Epilepsy Curr. 13 (Suppl. 1), 415.

Bonifacio, M.J., Sheridan, R.D., Parada, A., Cunha, R.A., Patmore, L., Soares-da-Silva, P., 2001. Interaction of the novel anticonvulsant, BIA 2-093, with voltage-gated sodium channels: comparison with carbamazepine. Epilepsia 42, 600–608.

Brady, K., Hebeisen, S., Konrad, D., Soares-da-Silva, P., 2011. The effects of eslicarbazepine, R-licarbazepine, oxcarbazepine and carbamazepine on ion transmission $Ca_v3.2$ channels. Epilepsia 52 (Suppl. 6), 260.

Brodie, M.J., Sills, G.J., 2011. Combining antiepileptic drugs–rational polytherapy? Seizure 20, 369–375.

Catterall, W.A., 1999. Molecular properties of brain sodium channels: an important target for anticonvulsant drugs. Adv. Neurol. 79, 441–456.

Chen, Y., Yu, F.H., Surmeier, D.J., Scheuer, T., Catterall, W.A., 2006. Neuromodulation of Na^+ channel slow inactivation via cAMP-dependent protein kinase and protein kinase C. Neuron 49, 409–420.
Doty, P., Rudd, G.D., Stoehr, T., Thomas, D., 2007. Lacosamide. Neurotherapeutics 4, 145–148.
Eijkelkamp, N., Linley, J.E., Baker, M.D., Minett, M.S., Cregg, R., Werdehausen, R., Rugiero, F., Wood, J.N., 2012. Neurological perspectives on voltage-gated sodium channels. Brain 135, 2585–2612.
Elger, C., Bialer, M., Falcao, A., Vaz-da-Silva, M., Nunes, T., Almeida, L., Soares-da-Silva, P., 2013. Pharmacokinetics and tolerability of eslicarbazepine acetate and oxcarbazepine at steady state in healthy volunteers. Epilepsia 54, 1453–1461.
Errington, A.C., Stohr, T., Heers, C., Lees, G., 2008. The investigational anticonvulsant lacosamide selectively enhances slow inactivation of voltage-gated sodium channels. Mol. Pharmacol. 73, 157–169.
Falcao, A., Maia, J., Almeida, L., Mazur, D., Gellert, M., Soares-da-Silva, P., 2007. Effect of gender on the pharmacokinetics of eslicarbazepine acetate (BIA 2-093), a new voltage-gated sodium channel blocker. Biopharm. Drug Dispos. 28, 249–256.
Gil-Nagel, A., Elger, C., Ben-Menachem, E., Halasz, P., Lopes-Lima, J., Gabbai, A.A., Nunes, T., Falcao, A., Almeida, L., Soares-da-Silva, P., 2013. Efficacy and safety of eslicarbazepine acetate as add-on treatment in patients with focal-onset seizures: integrated analysis of pooled data from double-blind phase III clinical studies. Epilepsia 54, 98–107.
Goldin, A.L., 2003. Mechanisms of sodium channel inactivation. Curr. Opin. Neurobiol. 13, 284–290.
Halasz, P., Cramer, J.A., Hodoba, D., Czlonkowska, A., Guekht, A., Maia, J., Elger, C., Almeida, L., Soares-da-Silva, P., 2010. Long-term efficacy and safety of eslicarbazepine acetate: results of a 1-year open-label extension study in partial-onset seizures in adults with epilepsy. Epilepsia 51, 1963–1969.
Hebeisen, S., Brady, K., Konrad, D., Soares-da-Silva, P., 2011. Inhibitory effects of eslicarbazepine acetate and its metabolites against neuronal voltage-gated sodium channels. Epilepsia 52 (Suppl. 6), 257–258.
Hufnagel, A., Ben-Menachem, E., Gabbai, A.A., Falcao, A., Almeida, L., Soares-da-Silva, P., 2013. Long-term safety and efficacy of eslicarbazepine acetate as adjunctive therapy in the treatment of partial-onset seizures in adults with epilepsy: results of a 1-year open-label extension study. Epilepsy Res. 103, 262–269.
Kwan, P., Brodie, M.J., 2006. Combination therapy in epilepsy: when and what to use. Drugs 66, 1817–1829.
Lees, G., Stohr, T., Errington, A.C., 2006. Stereoselective effects of the novel anticonvulsant lacosamide against 4-AP induced epileptiform activity in rat visual cortex in vitro. Neuropharmacology 50, 98–110.
Lipkind, G.M., Fozzard, H.A., 2010. Molecular model of anticonvulsant drug binding to the voltage-gated sodium channel inner pore. Mol. Pharmacol. 78, 631–638.
Loureiro, A.I., Fernandes-Lopes, C., Bonifacio, M.J., Wright, L.C., Soares-da-Silva, P., 2011. Hepatic UDP-glucuronosyltransferase is responsible for eslicarbazepine glucuronidation. Drug Metab. Dispos. 39, 1486–1494.
Matsuki, N., Quandt, F.N., Ten Eick, R.E., Yeh, J.Z., 1984. Characterization of the block of sodium channels by phenytoin in mouse neuroblastoma cells. J. Pharmacol. Exp. Ther. 228, 523–530.
McCollum, I.J., Vilin, Y.Y., Spackman, E., Fujimoto, E., Ruben, P.C., 2003. Negatively charged residues adjacent to IFM motif in the DIII-DIV linker of hNa(V)1.4 differentially affect slow inactivation. FEBS Lett. 552, 163–169.
McIlwain, H., Bachelard, H.S., 1985. Biochemistry and the Central Nervous System. Churchill Livingstone, Edinburgh.
McPhee, J.C., Ragsdale, D.S., Scheuer, T., Catterall, W.A., 1994. A mutation in segment IVS6 disrupts fast inactivation of sodium channels. Proc. Natl. Acad. Sci. U. S. A. 91, 12346–12350.
McPhee, J.C., Ragsdale, D.S., Scheuer, T., Catterall, W.A., 1998. A critical role for the S4-S5 intracellular loop in domain IV of the sodium channel alpha-subunit in fast inactivation. J. Biol. Chem. 273, 1121–1129.
Milovan, D., Almeida, L., Romach, M.K., Nunes, T., Rocha, J.F., Sokowloska, M., Sellers, E.M., Soares-da-Silva, P., 2010. Effect of eslicarbazepine acetate and oxcarbazepine on cognition and psychomotor function in healthy volunteers. Epilepsy Behav. 18, 366–373.
Niespodziany, I., Leclere, N., Vandenplas, C., Foerch, P., Wolff, C., 2013. Comparative study of lacosamide and classical sodium channel blocking antiepileptic drugs on sodium channel slow inactivation. J. Neurosci. Res. 91, 436–443.
Nunes, T., Rocha, J.F., Falcao, A., Almeida, L., Soares-da-Silva, P., 2013. Steady-state plasma and cerebrospinal fluid pharmacokinetics and tolerability of eslicarbazepine acetate and oxcarbazepine in healthy volunteers. Epilepsia 54, 108–116.
O'Reilly, J.P., Wang, S.Y., Wang, G.K., 2001. Residue-specific effects on slow inactivation at V787 in D2-S6 of Na(v)1.4 sodium channels. Biophys. J. 81, 2100–2111.
Perucca, E., Elger, C., Halasz, P., Falcao, A., Almeida, L., Soares-da-Silva, P., 2011. Pharmacokinetics of eslicarbazepine acetate at steady-state in adults with partial-onset seizures. Epilepsy Res. 96, 132–139.
Pratt, J.H., Berry, J.F., Kaye, B., Goetz, F.C., 1969. Lipid class and fatty acid composition of rat brain and sciatic nerve in alloxan diabetes. Diabetes 18, 556–561.
Quandt, F.N., 1988. Modification of slow inactivation of single sodium channels by phenytoin in neuroblastoma cells. Mol. Pharmacol. 34, 557–565.
Rogawski, M.A., Loscher, W., 2004. The neurobiology of antiepileptic drugs. Nat. Rev. Neurosci. 5, 553–564.
Ross, F.M., Gwyn, P., Spanswick, D., Davies, S.N., 2000. Carbenoxolone depresses spontaneous epileptiform activity in the CA1 region of rat hippocampal slices. Neuroscience 100, 789–796.
Sake, J.K., Hebert, D., Isojarvi, J., Doty, P., De Backer, M., Davies, K., Eggert-Formella, A., Zackheim, J., 2010. A pooled analysis of lacosamide clinical trial data grouped by mechanism of action of concomitant antiepileptic drugs. CNS Drugs 24, 1055–1068.
Stafstrom, C.E., 2010. Mechanisms of action of antiepileptic drugs: the search for synergy. Curr. Opin. Neurol. 23, 157–163.
Ulbricht, W., 2005. Sodium channel inactivation: molecular determinants and modulation. Physiol. Rev. 85, 1271–1301.
Vilin, Y.Y., Ruben, P.C., 2001. Slow inactivation in voltage-gated sodium channels: molecular substrates and contributions to channelopathies. Cell Biochem. Biophys. 35, 171–190.
West, J.W., Patton, D.E., Scheuer, T., Wang, Y., Goldin, A.L., Catterall, W.A., 1992. A cluster of hydrophobic amino acid residues required for fast Na(+)-channel inactivation. Proc. Natl. Acad. Sci. U. S. A. 89, 10910–10914.
Xiong, W., Li, R.A., Tian, Y., Tomaselli, G.F., 2003. Molecular motions of the outer ring of charge of the sodium channel: do they couple to slow inactivation? J. Gen. Physiol. 122, 323–332.